Collisionless and Hydrodynamic Excitations of a Bose-Einstein Condensate

D. M. Stamper-Kurn, H.-J. Miesner, S. Inouye, M. R. Andrews,* and W. Ketterle

*Department of Physics and Research Laboratory of Electronics, Massachusetts Institute of Technology,
Cambridge, Massachusetts 02139*

Collective excitations of a dilute Bose gas were probed above and below the Bose-Einstein condensation temperature. The temperature dependencies of the frequency and damping rates of condensate oscillations indicate significant interactions between the condensate and the thermal cloud. Hydrodynamic oscillations of the thermal cloud analogous to first sound were observed. An out-of-phase dipolar oscillation of the thermal cloud and the condensate was also studied, analogous to second sound. The excitations were observed *in situ* using nondestructive imaging techniques. [S0031-9007(98)06661-7]

Bose-Einstein condensation in dilute atomic gases [1–3] has provided a testing ground for well-developed many-body theories of quantum fluids. Many studies have focused on the collective excitations of such gases. Experiments have studied low-lying collective excitations over a range of temperatures [4–6] and higher-lying modes [7]. Zero-temperature findings have agreed well with predictions based on a mean-field description of the weak interatomic interactions [8–10]. However, the behavior at nonzero temperature, which involves interactions between the condensate and the thermal cloud, is not fully understood, pointing to the need for new theoretical developments.

The physical nature of collective excitations depends on the hierarchy of three length scales: the wavelength of the excitation λ, the healing length ξ which is given by the condensate density n_0 and the scattering length a as $\xi = (8\pi a n_0)^{-1/2}$, and the mean-free path l_{mfp} for collisions between the collective excitation and other excitations which compose the thermal cloud. The collisionless regime, defined by $\lambda \ll l_{mfp}$ (or by $\omega\tau \gg 1$ where ω is the frequency of the excitation and τ its collision time), occurs at zero temperature and for low densities of the thermal cloud. There, free-particle excitations are obtained at short wavelengths ($\lambda \ll \xi$), while phononlike excitations known as Bogoliubov sound (also referred to as zero sound in recent literature) are obtained at long wavelengths ($\lambda \gg \xi$) [11]. For excitations where λ is comparable to the size of the sample, this latter condition defines the Thomas-Fermi regime. Experiments have been performed either in the limit of Bogoliubov sound excitations [5,7] or intermediate to the two limits [4,6].

At higher densities of the normal component, when $\lambda \gg l_{mfp}$ ($\omega\tau \ll 1$), collective excitations become hydrodynamic in nature, and one expects two phononlike excitations, which are the in-phase or out-of-phase oscillations of two fluids (the normal fraction and the superfluid). The presence of two hydrodynamic modes is similar to the case of superfluid ^{4}He, where they are known as first and sec-

ond sound. However, in superfluid ^{4}He both fluids participate equally in first and second sound, while in a dilute Bose gas the oscillations of each fluid are nearly uncoupled: the in-phase oscillation involves mainly the thermal cloud, whereas the out-of-phase mode is confined mainly to the condensate [11,12].

In this Letter, we study collective excitations at nonzero temperature, and extend earlier work [6] in several ways. First, we study condensate oscillations entirely in the Thomas-Fermi regime. In contrast, results of Ref. [6] were complicated by the transition of the condensate from the Thomas-Fermi to the free-particle regime with increasing temperature. Second, near the critical temperature we approach the hydrodynamic limit and observe the onset of hydrodynamic excitations of the thermal cloud, analogous to first sound. Finally, we observe a new out-of-phase dipolar oscillation of the condensate and the thermal cloud, analogous to the out-of-phase second sound mode in liquid helium [12].

The excitations were probed generally in three steps. First, as described in a previous paper [13], we produced a magnetically confined, ultracold gas of atomic sodium in an equilibrium state which was controlled by changing the final frequency used in rf-evaporative cooling. The clouds were cigar shaped with weak confinement along one direction (axial) and tight confinement in the other two (radial). Second, the cloud was manipulated with either time-dependent magnetic fields or off-resonant light to excite low-lying collective modes. Finally, the cloud was allowed to oscillate freely and probed *in situ* with repeated, nondestructive phase-contrast imaging [7].

To accurately characterize the magnetic trapping potential, we excited center-of-mass oscillations of the cloud in the axial direction by sinusoidally moving the trap center. The subsequent free oscillation of the cloud gave the axial trapping frequency as $\nu_z = 16.93(2)$ Hz. The radial frequency was estimated to be 230(20) Hz.

The $m = 0$ quadrupolar modes of the condensate and the thermal cloud [5] were excited by a 5-cycle pulsed

modulation of the axial magnetic field curvature. Data were evaluated for oscillations with a relative amplitude of about 10% [14]. The oscillations of each cloud were probed with 22 nondestructive images: one before the excitation to characterize the initial conditions and three groups of 7 images during the free oscillation. The three groups were separated by a delay time which was varied between 1 and 200 ms according to the damping time of the oscillation. This method of probing gave highly accurate single-shot measurements of oscillation frequencies and damping rates, and overcame the additional fluctuations introduced when combining data from observations on several clouds.

Phase-contrast images were analyzed by fitting the observed column densities $\tilde{n}(r,z)$ [15] with the function

$$\tilde{n}(r,z) = h_c \max\left(0, 1 - \frac{r^2}{(r_c/2)^2} - \frac{z^2}{(z_c/2)^2}\right)^{3/2}$$
$$+ h_t g_2\left[\exp\left(-\frac{r^2}{2(r_t/2)^2} - \frac{z^2}{2(z_t/2)^2}\right)\right]. \quad (1)$$

Here, r and z are the radial and axial coordinates, respectively, while r_c and z_c are the lengths of the condensate and r_t and z_t the rms diameters of the thermal cloud. The function g_2 is defined by $g_2(x) = \sum_{i=1}^{\infty} x^i/i^2$. Equation (1) is motivated by a simple model of the mixed cloud: a mean-field dominated condensate amid a saturated noncondensed ideal gas obeying Bose-Einstein statistics [16]. Since all quantities were allowed to vary independently (including the amplitudes h_c and h_t), Eq. (1) is an almost model-independent parametrization of a bimodal distribution: z_c is determined from the cusps of the bimodal distribution, and z_t from the thermal tails.

The initial conditions for the oscillation were characterized by the total number of atoms N, the temperature T, and the chemical potential μ. N was obtained by integrating the column density, while T and μ were determined from the fits by $k_B T = \pi^2 m \nu_z^2 z_t^2$ and $\mu = \pi^2 m \nu_z^2 z_c^2/2$, where k_B is Boltzmann's constant. We determined T by fitting the thermal wings alone. In addition, an approximate condensate number N_0 was determined by summing the column density which is ascribed to the condensate according to the fits [first line of Eq. (1)]. These conditions are shown in Fig. 1 as a function of $\Delta\nu_{\rm rf} = \nu_{\rm rf} - \nu_{\rm bot}$ where $\nu_{\rm rf}$ is the final frequency used in the rf evaporation, and $\nu_{\rm bot}$ is the resonant rf frequency for atoms at the bottom of the magnetic trap. The frequency $\nu_{\rm bot}$ remained constant within 20 kHz. The Bose-Einstein condensation transition was observed at $T \simeq 1.7$ μK with about 80×10^6 atoms. The temperature varied linearly with $\Delta\nu_{\rm rf}$, with a slope of 3.5 μK/MHz, and was measurable down to 0.5 μK. Reliable determinations of z_c (and μ) were obtained only below $\Delta\nu_{\rm rf} = 350$ kHz. For low $\Delta\nu_{\rm rf}$, $\mu/k_B \simeq 380$ nK, corresponding to $N_0 \simeq 15 \times 10^6$.

The lengths z_c and z_t were fit independently to decaying sinusoidal functions of time. We thus determined the frequency and damping rate (the inverse of the $1/e$ decay
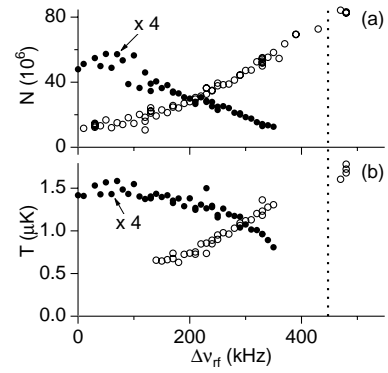

FIG. 1. Equilibrium conditions before excitation. The total number N [(a), open circles] was determined by summing over the observed column densities. The approximate condensate number N_0 [(a), closed circles, $\times 4$], temperature T [(b), open circles], and chemical potential μ/k_B [(b), closed circles, $\times 4$] were determined from fits to the data. These are plotted against $\Delta\nu_{\rm rf}$. The dashed line indicates the observed transition temperature. We estimate systematic errors in N and N_0 of as much as 20% due to the calibration of our phase-contrast signal.

time of the oscillation amplitude) of two distinct oscillations. We observed no evidence for coupling between the oscillations in z_c and in z_t, allowing one to consider the excitations as nearly isolated oscillations of the thermal cloud and of the condensate, respectively.

The thermal cloud oscillated at a frequency of about $1.75\nu_z$ with a damping rate of about 20 s^{-1} (Fig. 2). The observed frequency ν is between the predicted collisionless limit of $\nu = 2\nu_z$ and the hydrodynamic limit of $\nu = 1.55\nu_z$ [17]. The damping rate is predicted to vanish in both the collisionless and hydrodynamic limits, and to reach a broad maximum of $\sim 1.4\nu$ when ν is between its two limiting values [18], as we observe. One can estimate the collisional mean-free path as $l_{\rm mfp} \simeq (n_T\sigma)^{-1} = 96$ μm $\times (T/\mu{\rm K})^{-3/2}$ using the peak density of the thermal cloud $n_T = 2.612(mk_B T/2\pi\hbar^2)^{3/2}$, and a collisional cross section $\sigma = 8\pi a^2$ with the scattering length $a = 2.75$ nm [19]. Around the transition temperature, we find $z_t \simeq 8l_{\rm mfp}$. This comparison of length scales, the observed frequency shift away from $2\nu_z$, and the high damping rate all demonstrate that the collective behavior of the thermal cloud is strongly affected by collisions. Thus, the oscillations which we observe indicate the onset of hydrodynamic excitations. The hydrodynamic limit, characterized by low damping, would only be reached for even larger clouds.

We studied the $m = 0$ quadrupolar condensate oscillations in greater detail. Typical oscillation data (Fig. 3) demonstrate that the oscillation has a slightly lower frequency and is damped more rapidly at high temperature than at low temperature. At low temperatures, the condensate oscillation frequency approached a limiting value of $1.569(4)\nu_z$, close to the zero-temperature, high-density
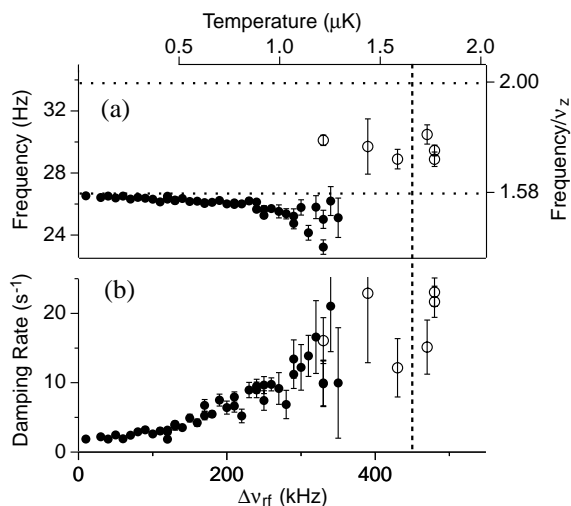
FIG. 2.   Temperature dependent frequency and damping rates of $m = 0$ quadrupolar collective modes. Points show measurements for oscillations of the thermal cloud (open circles) and condensate (closed circles). The free-particle limit of $2\nu_z$ and the zero-temperature condensate oscillation limit of $1.580\nu_z$ are indicated. The vertical dashed line marks the observed transition temperature. The temperature axis is based on a linear fit to the data in (b), and is determined only for $T > 0.5$ μK, where temperature could be measured.
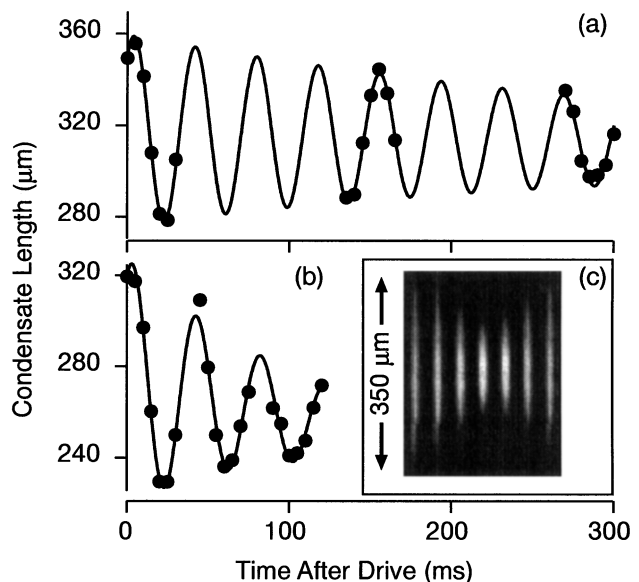

FIG. 3.   Quadrupolar condensate oscillations. Axial condensate lengths determined from fits to phase-contrast images are shown for (a) low and (b) high temperature. (a) $\Delta\nu_{\rm rf} = 30$ kHz and $T < 0.5$ μK; (b) $\Delta\nu_{\rm rf} = 250$ kHz and $T = 0.95$ μK. Lines are fits to a damped sinusoidal oscillation with a downward slope to account for heating. (c) *In situ* images, taken at 5 ms intervals, show large-amplitude oscillations of a low-temperature Bose-Einstein condensate. Final data were evaluated for oscillation amplitudes of about 10%.

prediction of $1.580\nu_z$ [9]. The slight difference between these values may be due to nonzero-temperature effects even for small $\Delta\nu_{\rm rf}$. At higher temperatures, the frequency drops below the low-temperature limit. This trend might be explained by the weakening of the effective trapping potential for the condensate by the mean-field potential of the thermal cloud. Considering a thermal density $n_T \propto e^{-U(r,z)/k_BT}$, one can estimate a downward frequency shift of as much as 5% due to this effect, consistent with our observations.

Damping rates for the condensate oscillations varied strongly with temperature, rising from a low-temperature limit of about 2 s^{-1} to as much as 20 s^{-1}. Recent treatments based on Landau damping [20–22] provide qualitative agreement with our findings. A quantitative prediction for these damping rates [22] could not be checked because our data were collected for $k_BT \lesssim 6\mu$, where the high-temperature prediction might not be applicable, while the inability to measure T for low $\Delta\nu_{\rm rf}$ prevents a comparison at low temperatures.

For the condensate oscillations at high temperatures, a comparison of length scales ($z_c \simeq 4\,l_{\rm mfp}$) indicates that hydrodynamic effects may already be present. This suggests that these oscillations may constitute second sound in a Bose gas [11]. However, there are no theoretical predictions regarding the transition from collisionless to hydrodynamic condensate oscillations with which to compare our data. In future experiments with larger condensates, the signature of this crossover may appear in the damping rate of the oscillations, which should decrease

again at high temperatures as one reaches the hydrodynamic limit.

To further probe the interaction between the thermal cloud and the condensate, we studied an excitation of a different symmetry: the rigid-body, out-of-phase motion of the condensate and the thermal cloud in the harmonic trapping potential [12]. This mode is analogous to second sound in liquid helium, where the superfluid and the normal fluid undergo out-of-phase density oscillations of equal magnitude.

We excited this mode with focused off-resonant, blue-detuned laser light, which produced a 3-μK-high repulsive potential similar to that used in Ref. [7]. After a partly condensed cloud was formed, the light was turned on and directed at the edge of the cloud, where it overlapped only with the thermal cloud. By tilting a motorized mirror, the laser beam was steered toward and then away from the center of the cloud, pushing the thermal cloud in the axial direction while not directly affecting the condensate. The light was then turned off, and the cloud allowed to freely oscillate.

The position of the center of mass of the condensate [Fig. 4(a)] was monitored with repeated phase-contrast images. The condensate motion was initially slow, and then grew to an asymptotic sinusoidal oscillation, corresponding to the in-phase motion of the entire cloud (condensate plus thermal cloud) at the trapping frequency ν_z. By subtracting the undamped center-of-mass motion of the entire
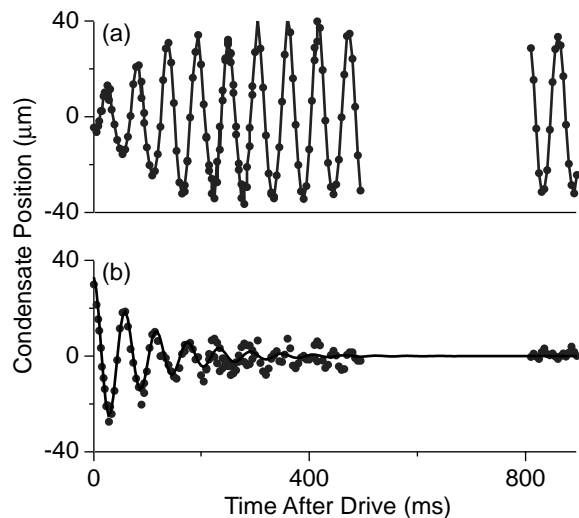
FIG. 4.   Out-of-phase dipole mode of a partly condensed cloud. The center-of-mass of the condensate in the trap (a) was monitored after displacing the thermal cloud with a far-detuned laser beam. The condensate oscillated relative to the center-of-mass of the entire sample (b) at a frequency smaller than ν_z, with a damping rate of $9(1)$ s^{-1}. The line in (a) is a guide to the eye, and that in (b) is a fit to the data. Data were collected in several repetitions of the experiment, for which $T = 1$ μK, $\mu/k_B = 200$ nK, and $N = 40 \times 10^6$.

cloud, we isolated the out-of-phase oscillation of the condensate and the thermal cloud [Fig. 4(b)].

The frequency of the out-of-phase dipole mode of 17.26(9) Hz was significantly lower than the trapping frequency which was $\nu_z = 18.04(1)$ Hz at that time. This $\sim 5\%$ frequency shift is again evidence of the interaction between the thermal cloud and the condensate. The motion we observed, in which the condensate is driven by the moving thermal cloud, cannot be described by recent theories which assume a stationary thermal cloud [23], and requires more sophisticated treatments [12,21].

In conclusion, we have studied the collective excitations of a dilute Bose gas at nonzero temperatures in the Thomas-Fermi limit, and near the hydrodynamic regime. The hydrodynamic oscillation of the thermal cloud, corresponding to first sound, was indicated by measurements both above and below the Bose-Einstein condensation transition. The accurately determined frequency shift of the $m = 0$ quadrupole oscillations away from their zero-temperature limit and of the out-of-phase oscillation away from the trap frequency are measures of the forces exerted by the condensate and the thermal cloud on one another.

*Present address: Bell Labs, Lucent Technologies, Murray Hill, NJ 07974.

[1] M. H. Anderson et al., Science **269**, 198 (1995).

[2] K. B. Davis et al., Phys. Rev. Lett. **75**, 3969 (1995).

[3] C. C. Bradley, C. A. Sackett, and R. G. Hulet, Phys. Rev. Lett. **78**, 985 (1997); see also C. C. Bradley et al., Phys. Rev. Lett. **75**, 1687 (1995).

[4] D. S. Jin et al., Phys. Rev. Lett. **77**, 420 (1996).

[5] M.-O. Mewes et al., Phys. Rev. Lett. **77**, 988 (1996).

[6] D. S. Jin et al., Phys. Rev. Lett. **78**, 764 (1997).

[7] M. R. Andrews et al., Phys. Rev. Lett. **79**, 553 (1997).

[8] M. Edwards et al., Phys. Rev. Lett. **77**, 1671 (1996).

[9] S. Stringari, Phys. Rev. Lett. **77**, 2360 (1996).

[10] E. Zaremba, Phys. Rev. A **57**, 518 (1998); G. M. Kavoulakis and C. J. Pethick, e-print cond-mat/9710130.

[11] T. D. Lee and C. N. Yang, Phys. Rev. **113**, 1406 (1959); A. Griffin, *Excitations in a Bose-Condensed Liquid* (Cambridge University Press, Cambridge, 1993), and references therein; A. Griffin and E. Zaremba, Phys. Rev. A **56**, 4839 (1997); V. B. Shenoy and T.-L. Ho, Phys. Rev. Lett. **80**, 3895 (1998).

[12] E. Zaremba, A. Griffin, and E. Nikuni, e-print cond-mat/9705134.

[13] M.-O. Mewes et al., Phys. Rev. Lett. **77**, 416 (1996).

[14] The condensate oscillation frequency rose by as much as 1 Hz from its low-amplitude limit as the relative amplitude of oscillation increased from 10% to 50%. This shift agrees with predictions of F. Dalfovo, C. Minniti, and L. P. Pitaevskii, Phys. Rev. A **56**, 4855 (1997).

[15] A phase-contrast image gives the optical phase ϕ accrued by off-resonant light passing through a dense medium. For our setup, the column density $\tilde{n} = \phi \times 6.2 \times 10^{11}$ cm^{-2}.

[16] V. Bagnato, D. E. Pritchard, and D. Kleppner, Phys. Rev. A **35**, 4354 (1987).

[17] A. Griffin, W.-C. Wu, and S. Stringari, Phys. Rev. Lett. **78**, 1838 (1997); Yu. Kagan, E. L. Surkov, and G. V. Shlyapnikov, Phys. Rev. A **55**, R18 (1997).

[18] G. M. Kavoulakis, C. J. Pethick, and H. Smith, Phys. Rev. A **57**, 2938 (1998).

[19] E. Tiesinga et al., J. Res. Natl. Inst. Stand. Technol. **101**, 505 (1996).

[20] W. V. Liu, Phys. Rev. Lett. **79**, 4056 (1997); L. P. Pitaevskii and S. Stringari, Phys. Lett. A **235**, 398 (1997).

[21] S. Giorgini, Phys. Rev. A **57**, 2949 (1998).

[22] P. O. Fedichev, G. V. Shlyapnikov, and J. T. M. Walraven, Phys. Rev. Lett. **80**, 2269 (1998).

[23] D. A. W. Hutchinson, E. Zaremba, and A. Griffin, Phys. Rev. Lett. **78**, 1842 (1997); R. J. Dodd, M. Edwards, C. W. Clark, and K. Burnett, Phys. Rev. A **57**, R32 (1998).